

RECEIVED

MAR 27 1996

OSTI

RRB
ANL/PHY/CP--89¹₅₀₄
CONF-950127-15

Measuring two-particle Bose-Einstein correlations with
PHOBOS@RHIC

Gunther Roland for the PHOBOS collaboration

Argonne National Laboratory

R. Betts

Brookhaven National Laboratory

D. Barton, A. Carroll, Y.Y. Chu, S. Gushue, H.W. Kraner, L.P. Remsberg

Institute of Nuclear Physics, Krakow

A. Budzanowski, T. Coghen, R. Hołynski, J. Kotuła, H. Palarczyk, P. Malecki,
A. Olszewski, K. Pakoński, M. Stodulski, A. Trzupek, H. Wilczyński, B. Wosiek,
K. Woźniak, K. Zalewski

Jagiellonian University, Krakow

A. Białas, W. Czyż

Massachusetts Institute of Technology

M.D. Baker, W. Busza, P. Kulinich, M. Płesko, G. Roland, L. Rosenberg, J.J. Ryan,
S.G. Steadman, P. Steinberg, G.S.F. Stephans, R. Verdier, B. Wadsworth, D. Woodruff,
B. Wysłouch

Oak Ridge National Laboratory

C. Britton

University of Illinois at Chicago

C. Conner, C. Halliwell, D. McLeod

University of Maryland

A. Mignerey, J. Shea

Yale University

S. Manly

We present results of a simulation of the measurement of two-particle Bose-Einstein correlations in central Au-Au collisions with the PHOBOS detector at RHIC. This measurement is expected to yield information on the relevant time and distance scales in these collisions. As the space-time scale is directly connected with the equation of state governing the evolution of the particle source, this information will be essential in understanding the physics of nucleus-nucleus collisions at RHIC energies. We demonstrate that the PHOBOS detector has sufficient resolution and acceptance to distinguish a variety of physics scenarios.

MASTER

DISTRIBUTION OF THIS DOCUMENT IS UNLIMITED *al*

The submitted manuscript has been authored by a contractor of the U. S. Government under contract No. W-31-109-ENG-38. Accordingly, the U. S. Government retains a nonexclusive, royalty-free license to publish or reproduce the published form of this contribution, or allow others to do so, for U. S. Government purposes.

DISCLAIMER

This report was prepared as an account of work sponsored by an agency of the United States Government. Neither the United States Government nor any agency thereof, nor any of their employees, makes any warranty, express or implied, or assumes any legal liability or responsibility for the accuracy, completeness, or usefulness of any information, apparatus, product, or process disclosed, or represents that its use would not infringe privately owned rights. Reference herein to any specific commercial product, process, or service by trade name, trademark, manufacturer, or otherwise does not necessarily constitute or imply its endorsement, recommendation, or favoring by the United States Government or any agency thereof. The views and opinions of authors expressed herein do not necessarily state or reflect those of the United States Government or any agency thereof.

DISCLAIMER

**Portions of this document may be illegible
in electronic image products. Images are
produced from the best available original
document.**

1. Introduction

The measurement of two-particle Bose-Einstein correlations (called HBT-measurement in the following) is the most important tool for obtaining information on the space-time evolution of the extended hadron source created in ultrarelativistic heavy ion collisions [1-4]. The experimental observable in this study is the two-particle correlation function for pairs of identical bosons. It is defined as the ratio of the two-particle inclusive distribution for particles with momenta k_1 and k_2 , divided by the product of the single particle inclusive distributions:

$$C_2(k_1, k_2) = \frac{P_2(k_1, k_2)}{P_1(k_1) \cdot P_1(k_2)}. \quad (1)$$

For identical bosons the correlation function is enhanced at low relative momenta and the width of the enhancement region in momentum space is inversely proportional to a typical length scale (called the 'HBT radius') of the particle source. For a static thermal source this length scale (or radius) is given by the geometrical size of the source. In general however the length scale will be influenced by so-called dynamical correlations, which lead to a correlation between position and momentum of the particles at freeze-out. The most important type of dynamical correlations are those caused by a rapid expansion of the particle source. In this case a dependence of the effective radii (corresponding to different components of the momentum difference \vec{Q}) on the longitudinal and transverse momentum of the particles is introduced. The dynamical correlations therefore link the observables studied in the analysis of two-particle correlations to the dynamics of the expansion of the particle source. The expansion in turn is governed by the equation of state of the strongly interacting matter produced in the collision. A definition of the different HBT parameters and a detailed description of the connection between the space-time parameters of the particle emission and the HBT parameters can be found in [5]. One of the main aims of the PHOBOS experiment is to study the correlation function as a function of all relevant degrees of freedom in momentum space for pions and kaons.

2. The PHOBOS detector

The PHOBOS detector consists of two main components [6]: One is a 4π multiplicity array that measures the angular distribution of charged particles and (to some extent) photons. The other part is a two arm magnetic spectrometer near mid-rapidity. The spectrometer provides momentum analysis and particle identification in the $1/\beta^2$ region for about 1 % of all charged particles. Though not part of the PHOBOS baseline design, we expect to use a Time-of-flight wall to extend the particle identification capabilities to higher momenta.

The most important aspect of the PHOBOS design is that all detector elements are produced in a common technology, namely as Silicon Pad detectors and are read out by one type of electronics. We will use a total of around 80.000 detector channels. The simplicity of the PHOBOS design should enable us to quickly debug and understand our detector at RHIC startup.

One consequence of the technology choice made for PHOBOS is that the size and relative position of the basic detector pixel are determined solely by the production of

expansion
 \vec{Q}_{LONG}
 \vec{Q}_{TRANS}

the Si wafers and are not subject to any further calibration. This is a substantial difference compared to other charged particle detectors where the charge deposited by an ionizing particle is drifting to a readout anode over some distance. In the context of this paper the fact that the PHOBOS position resolution is essentially calibration-free ensures that the estimates we obtain from the detector simulation will actually apply to the real detector. Another important factor for the PHOBOS HBT studies is the very high rate capability of our Silicon Pad detectors and the readout chain, which will allow us to record all central events occurring within ± 10 cm of the nominal interaction point, without any bias.

3. Pattern Recognition

A meaningful assessment of the HBT capabilities of a detector in the high particle density environment of high energy nucleus-nucleus collisions can only be obtained by studying the performance of a *full pattern recognition chain* on simulated detector data. Only in this way one can obtain the necessary information about complex questions like the two track resolution or the distribution of ghost tracks in relative momentum space. We have developed a complete pattern recognition chain that starts from the raw pixeled detector hits in high multiplicity events and performs the necessary pattern recognition and momentum determination steps and also does particle identification by energy loss measurements in the $1/\beta^2$ region.

The particular pattern recognition algorithm that we have employed for this study consists of the following steps:

First track candidates are independently formed in two regions of the spectrometer. For hits in the first 6 planes, which lie outside the magnetic field, a Hough transformation of the hit coordinates into a two-dimensional space given by the polar and azimuthal angles Θ and ϕ is performed. For the planes inside the magnetic field a similar transformation is done for *pairs* of hits in adjacent planes, this time into Θ and $1/p$, where p is the total momentum of the particles. In this way hits on tracks originating at the vertex are transformed into clusters of hits in (Θ, ϕ) and $(\Theta, 1/p)$ space, respectively. Based on these hit-clusters straight line and curved track candidates are formed. One should note that this method does not imply any approximation regarding the shape or uniformity of the magnetic field and can be based on look-up tables, thus making it very cpu time-efficient.

In the next step full candidate tracks are formed by matching straight line and curved track candidates based on the polar angle Θ and on the limited ϕ information that is available from the coarse vertical segmentation of the planes inside the magnetic field. For the low-momentum tracks (e.g. pions with $p < 250$ MeV/c) it has turned out to be necessary to also include the dE/dx particle ID information at this step.

The track candidates are then subjected to a χ^2 -fit and those with a χ^2 -probability of less than 3 % are rejected. To achieve the PHOBOS goal of measuring tracks with very low momenta it was essential to use the full covariance matrix in this fit, to account for the correlation in the fit residuals due to multiple scattering. As mentioned before, the fact that the PHOBOS position resolution is calibration-free assures that we will also have a sufficient understanding of the fit residuals for the real detector to apply this method.

In the final step successful track candidates are checked for shared hits and in case of conflicting candidates the one with the better χ^2 is retained. In this step another check

is done for potential close ghost-pairs, i.e. pairs that are close in momentum space and were created out of the same input track plus a number of alien hits.

In the following a 'Ghost track' is defined as an output track that shares less than 8 out of a possible 11 hits with an input track or has a momentum that is more than 5% different from that of the corresponding input track. Only one output track is allowed to be matched to any given input track. This criterion ensures that all the 'true' found tracks have both momentum and PID-characteristics close to the corresponding input track.

4. Performance

In this section we will discuss the performance of the PHOBOS pattern recognition for high multiplicity events with respect to the variables that are relevant for two-particle correlation measurements. In figs. 1 and 2 the p_T - y distributions for negatively charged pions and kaons originating from collisions at the nominal vertex position at $z = 0$ cm are shown. For the magnetic field configuration used here negative particles are bent towards the beampipe.

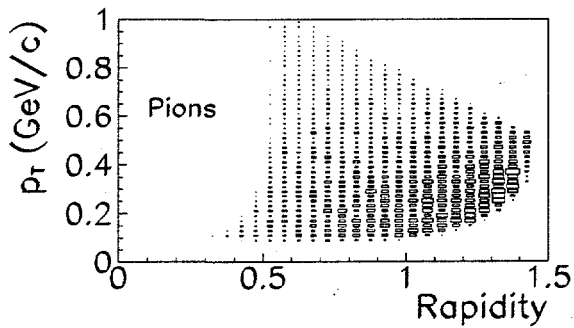


Figure 1. p_T - y distributions for reconstructed negative pions produced in collisions at $z = 0$ cm.

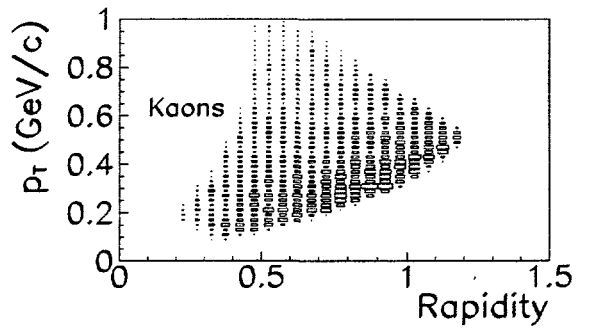


Figure 2. p_T - y distributions for reconstructed negative kaons produced in collisions at $z = 0$ cm.

The low momentum cutoff is given by the geometrical acceptance of the detector for these tracks (the particles were required to traverse all 11 planes of one detector arm) and the high momentum cutoff is determined by the limit of the TOF particle ID of approximately 1150 MeV/c. The width of the rapidity distribution for a *single* event is around one unit of rapidity. This fulfills one important requirement for HBT measurements, as a minimal acceptance in rapidity is needed to perform a reliable fit of the Q_{long} component of the correlation function, especially in a low p_T bin. Also, the expected correlation length for a locally thermalized particle source along the longitudinal axis is on the order of 0.5 rapidity units.

To investigate the correlation function in different rapidity regions and to extend the low- p_T coverage, PHOBOS will accept collisions over an interval of vertex positions ranging from -10 cm to 10 cm around the nominal interaction point. The corresponding p_T - y

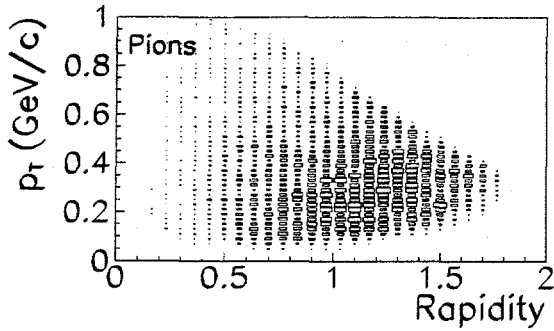


Figure 3. p_T - y distributions for reconstructed pions produced in collisions at $-10 < z < 10$ cm.

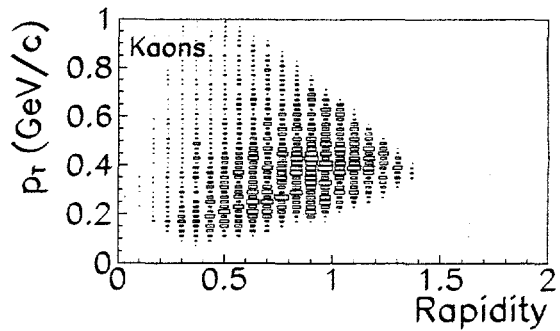


Figure 4. p_T - y distributions for reconstructed kaons produced in collisions at $-10 < z < 10$ cm.

distributions for pions and kaons of both charges are shown in figs. 3 and 4. Fig. 3 also demonstrates that the PHOBOS acceptance for pions indeed reaches down to very low transverse momenta of about 40 MeV/c.

The reconstruction efficiency of the PHOBOS detector was determined for tracks in central events, with an average primary charged particle multiplicity of 6000. To get a meaningful estimate of the overall efficiency and the production of false ('Ghost') tracks, the effects of multiple coulomb scattering and the hits of non-vertex tracks from weak decays of primary particles and secondary interactions were taken into account.

The resulting momentum and Θ distributions of found tracks and ghost tracks, together with the distributions of input tracks are shown in fig. 5. The lower plot in fig. 5 shows the ratios of the momentum distributions for found tracks over input tracks and ghost tracks over input tracks. For the present algorithm an average reconstruction efficiency of 76% was obtained, with a very low rate of ghost tracks of only 3-4%. We expect that with some fine tuning of the reconstruction algorithm an efficiency of 85-90% can be achieved with the same rate of ghost tracks. For the present study however the efficiency shown here was deemed sufficient, as the emphasis for two-particle correlation studies has to be on the two-particle acceptance as a function of relative momentum and especially on the suppression of artificial close pairs, which would distort the correlation function.

One of the most important questions for studying two-particle correlations is the distribution of ghost tracks in momentum space relative to other tracks. One has to keep in mind that for the large particle sources expected at RHIC HBT essentially becomes a very small effect. While a correction for two-particle efficiency is relatively straightforward it is in general not possible to reliably correct for artificial close pairs, once they have been created by the pattern recognition. Therefore fig. 6 provides a very important piece of information, showing that there is no pile-up of ghost pairs at low values of the invariant momentum difference Q_{inv} .

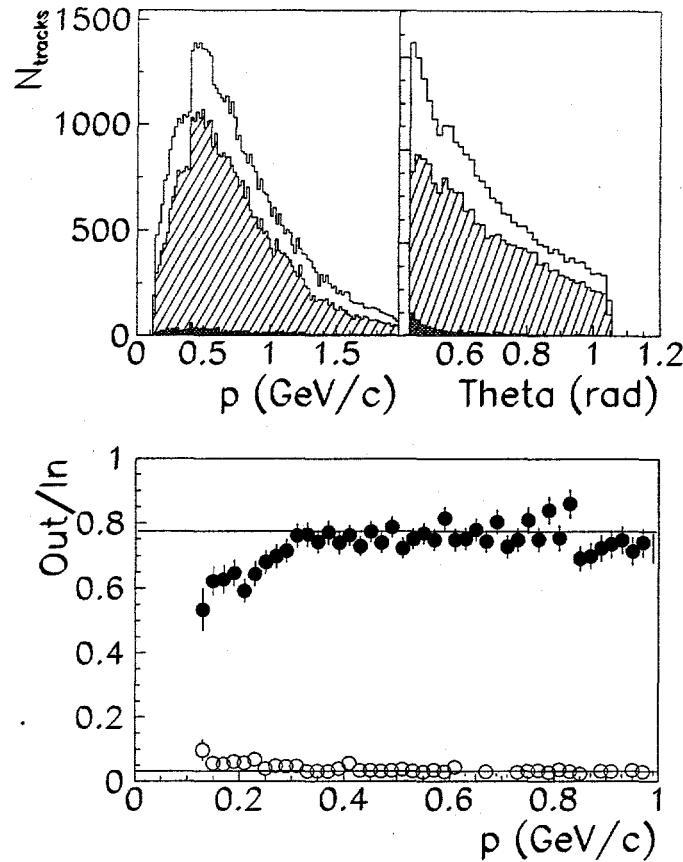


Figure 5. The upper plots show the momentum distribution (left) and Θ -distribution (right) for input tracks (solid line), correctly found tracks (dashed histogram) and ghost tracks (dark histogram). The lower plot shows the ratio of correctly found tracks to input tracks (full symbols) and ghost tracks to input tracks (open symbols).

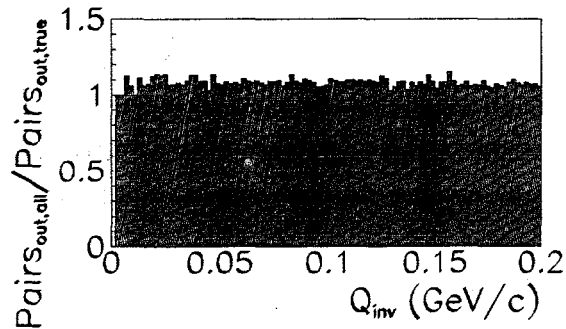


Figure 6. This plot shows the ratio of two Q_{inv} distributions. The numerator was formed using all output tracks of the pattern recognition, including ghost tracks. The denominator only includes 'true' output tracks. There is no excess of ghost pairs at low Q_{inv} .

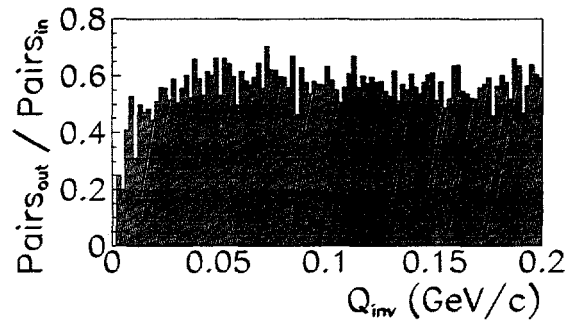


Figure 7. This plot shows the ratio of two Q_{inv} distributions. The numerator was formed using the output tracks of the pattern recognition, the denominator was formed using the input tracks.

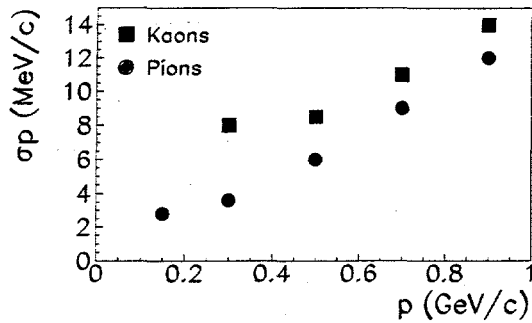


Figure 8. Average momentum error as a function of total momentum for pions (circles) and kaons (squares).

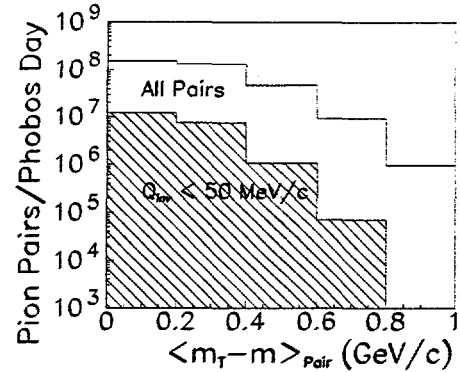


Figure 9. Number of pion pairs per day of PHOBOS running. The solid line shows the number of all pairs per m_T -bin, the dashed histogram shows the number of pairs with $Q_{inv} < 50$ MeV/c per m_T -bin.

In fig. 7 we show the two-track resolution obtained for the present pattern recognition chain. The two-track efficiency is constant (and equal to the square of the single particle efficiency) up to about 25 MeV/c and then gradually drops to about 50% of the plateau-value. For very large sources we will therefore need to apply a two-particle acceptance correction, which is a standard procedure in the study of two-particle correlations. Again the relative simplicity of the PHOBOS detector elements will ensure that we will be able to perform this correction with little uncertainty.

The momentum resolution that was achieved for tracks in high-multiplicity events is shown in fig. 8 as a function of momentum. For low momentum tracks the resolution is dominated by the effects of multiple scattering, which also guided our choice of the detector granularity.

In the final performance plot (fig. 9) we show the number of pion pairs measured in one day of PHOBOS running at the RHIC design luminosity for different bins of transverse momentum. Clearly the errors on the HBT parameters as measured by PHOBOS will be dominated by systematic errors arising from e.g. the uncertainties of the Coulomb correction or the fitting procedure, rather than the statistical errors.

5. Physics simulations

Here we will demonstrate the PHOBOS physics capabilities based on the performance figures that were shown in the previous section. We have studied the response of the PHOBOS detector to three very different physics scenarios that cover some part of the predictions of what is going to happen at RHIC. We did not try to include effects of resonance decays in the present study.

In performing the physics simulation we had to use a somewhat simplified approach.

The ideal solution would consist of using an event generator to generate a number of events that is comparable to that expected for one day of PHOBOS running at RHIC and symmetrize the momenta of all identical particles according to the distribution of emission points. This approach however is unfeasible as we don't yet have access to the computing power that will be needed for the simulation and analysis of such a number of events. Also symmetrising all the particle momenta in a high multiplicity event is a non-trivial problem.

We have therefore developed a HBT-simulation chain that is based on a parametrization of the PHOBOS two-particle acceptance and momentum resolution as obtained for high multiplicity events. Particles according to different space-time evolution scenarios were generated and combined to particle pairs. Using the code developed by S. Pratt (based on the Wigner-function formalism) [10], a weight for each pair was calculated according to the symmetrization requirements and the Coulomb repulsion between the two particles. The particle pairs are then passed through a simulation of the PHOBOS pair response. The correlation function is formed using weighted and non-weighted particle pairs and applying the standard Gamov penetration factor to account for the Coulomb repulsion. To extract values for the HBT radii, fits to the correlation functions were performed with the following functional form:

$$C_2 = 1 + \lambda \exp(-Q_{side}^2 R_{side}^2 - Q_{out}^2 R_{out}^2 - Q_{long}^2 R_{long}^2), \quad (2)$$

without a factor $\frac{1}{2}$ in the exponent. The statistics used in all three scenarios correspond to one day of running for the pions and one week of running for the kaons.

The first physics scenario is based on a straightforward extrapolation of HBT results that were obtained for collisions of heavy ions at SPS-energies. The HBT results at the SPS can be summarized as follows [5,7-9]:

- The transverse radii R_{side} scale as $dN/dy^{\frac{1}{3}}$. This leads to radii of the order of 10 fm for the expected multiplicity densities at RHIC.
- The longitudinal radius R_{long} shows the rapidity and p_T dependence expected for a scaling longitudinal expansion. The duration of the expansion is on the order of 4-5 fm/c. It follows a similar dN/dy -dependence as the transverse radius.
- There is a dependence of the transverse radius on p_T that seems to be somewhat weaker than for the longitudinal radius and can be explained by a combination of a weak transverse expansion and the p_T dependence of resonance contributions.
- For kaons significantly smaller radii have been observed than for pions.

The result of taking this 'standard' scenario and extrapolating to RHIC energies is shown in fig. 10. The points, showing the result from fitting the correlation function that was obtained for the simulated PHOBOS response, follow closely the results for an ideal detector, which are shown as solid lines. An example of a pion correlation function is shown in fig. 11. For this scenario PHOBOS allows a detailed quantitative analysis of the correlation function in all relevant degrees of freedom for both pions and kaons.

A second scenario that has been predicted for RHIC is that of a particle source rapidly expanding in longitudinal *and* transverse direction. This case has been investigated in a

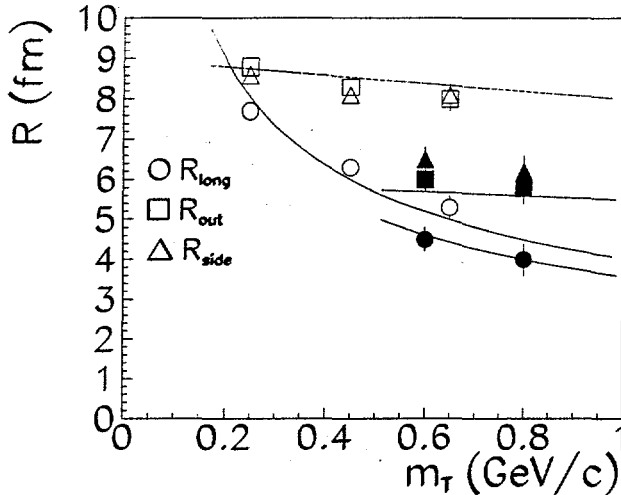


Figure 10. HBT radii for the 'standard' scenario. Points give the fitted radii including PHOBOS detector response; solid lines are radii for an 'ideal' detector. Open symbols are pions, full symbols are kaons.

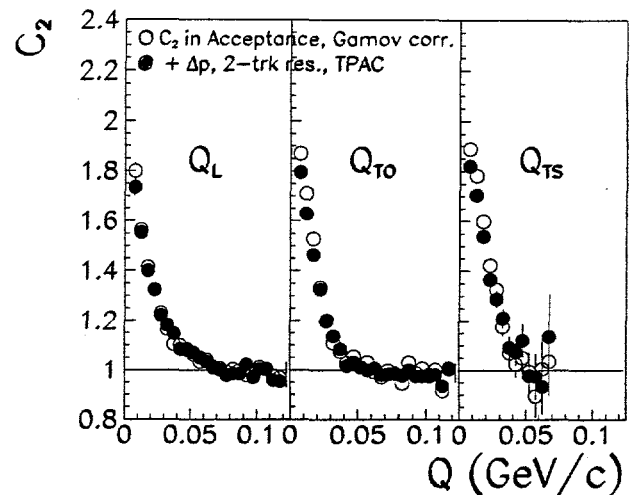


Figure 11. Projected pion correlation function for an ideal detector (open symbols) and the simulated PHOBOS response (full symbols).

recent paper by Csörgö and Lörstad [11]. They conclude that in this situation all three radii will show a common $1/\sqrt{m_T}$ dependence. The observed radii will not reflect the size of the particle source at freezeout (which may be very large) but will measure a common thermal correlation length. A possible signature of such a scenario is shown in fig. 12, where we assumed that kaon freezeout will occur earlier than pion freezeout.

This has to be compared to a third scenario, in which we assume a strong first phase transition with a large latent heat. In this case one expects a long lifetime of the particle source and a weak transverse expansion due to the 'softness' of the equation of state near the phase transition point. Only in the case of a very long source lifetime could one expect to obtain very large measured radii on the order of 20 fm. The PHOBOS response for this scenario is shown in fig. 13. Here we see that for the low transverse momentum bin, PHOBOS can accurately measure even very large radii, as we look at tracks of very low total momentum with a very small absolute momentum error of only a few MeV/c.

For the kaons the observed radii somewhat overshoot those for an ideal detector. One reason for this is that the Coulomb correction was performed using the standard Gamov factor, which leads to an overcorrection due to the finite size of the particle source. To reduce systematical errors caused by the Coulomb correction when real data will become available more theoretical work is required.

6. Conclusions

The measurement of two-particle Bose-Einstein correlations presents one of the few direct ways of probing the space-time evolution in ultra-relativistic heavy ion collisions. Using a detailed simulation of our detector and a full pattern recognition chain we have

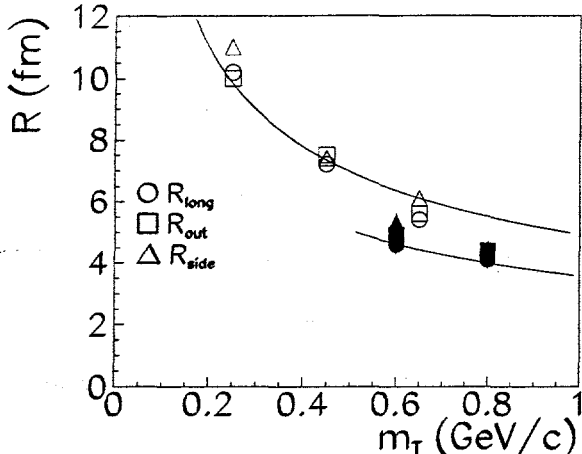


Figure 12. HBT radii for the 'rapid expansion' scenario. Points give the fitted radii including PHOBOS detector response; solid lines are radii for an 'ideal' detector. Open symbols are pions, full symbols are kaons.

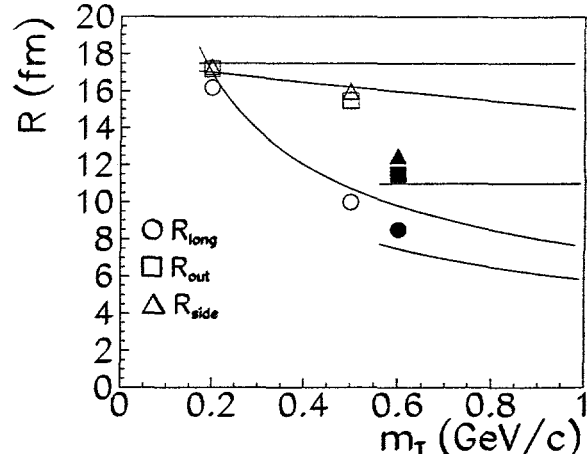


Figure 13. HBT radii for the 'long lifetime' scenario. Points give the fitted radii including PHOBOS detector response; solid lines are radii for an 'ideal' detector. Open symbols are pions, full symbols are kaons.

demonstrated that PHOBOS has the necessary resolution and acceptance to distinguish a variety of physics scenarios. The high rate capability ensures that we can perform a detailed investigation even for two-kaon correlations. The fact that PHOBOS is able to measure particles with small total momentum, allows for the observation of very large source sizes. Finally the simplicity of the PHOBOS design will help us in minimizing the systematical uncertainties of the HBT measurement. This work was supported by the U.S. Department of Energy, Nuclear Physics Division, under contract W-31-109-ENG-38.

REFERENCES

1. S. Pratt, Phys. Rev. **D33** (1986) 1314
2. G. Bertsch, M. Gong, M. Tohyama, Phys. Rev. **D37** (1988) 1896
3. K. Kolehmainen, M. Gyulassy, Phys. Lett. **180** (1986) 203
4. A. N. Mahklin, Yu. M. Sinyukhov, Z. Phys. Lett. **C39** (1988) 69
Yu. M. Sinyukhov, Nucl. Phys. **A498** (1989) 151
5. D. Ferenc et al. in 'Quark Matter '91', Nucl. Phys. **A544** (1992) 531
6. See also the contribution of M. Baker to these proceedings
7. G. Roland et al. Nucl. Phys. **A566** (1994) 527c
8. T. J. Humanic et al. Nucl. Phys. **A566** (1994) 115c
9. For a recent review see the contributions by Th. Alber et al. (NA35) and B. Jacak et al. (NA44) to the Quark Matter '95 conference, Monterey
10. S. Pratt, Th. Csörgö, J. Zymanyi, Phys. Rev. **C42** (1990) 2646
11. See Th. Csörgö's contribution to Quark Matter '95 conference, Monterey.